



Inorganic microporous membranes for hydrogen separation: Challenges and solutions

Ahui Hao, Xin Wan, Xiaofang Liu, Ronghai Yu, and Jianglan Shui (✉)

School of Materials Science and Engineering, Beihang University, Beijing 100191, China

Received: 27 April 2022 / Revised: 27 May 2022 / Accepted: 1 June 2022

ABSTRACT

Porous membrane separation is a competitive hydrogen purification technology due to the advantages of environmental friendliness, energy-saving, simple operation, and low cost. Benefiting from the booming development of materials science and chemical science, great progress has been made in H₂ separation with porous membranes. This review focuses on the latest advances in the design and fabrication of H₂ separation inorganic microporous membranes, with emphasis on the synthetic strategies to achieve structural integrity, continuity and stability. This review starts with a brief introduction to the membrane separation mechanisms, followed by an elaboration on the synthetic challenges and corresponding solutions of various high-performance inorganic microporous membranes based on zeolites, silica, carbon, and metal-organic frameworks (MOFs). At last, by highlighting the prospects of ultrathin two-dimensional (2D) porous membranes, we wish to shed some light on the further development of new materials and membranes for highly efficient hydrogen separation.

KEYWORDS

microporous membrane, H₂ separation, zeolite membrane, silica membrane, carbon membrane, metal-organic framework (MOF) membrane

1 Introduction

Hydrogen energy is an efficient and clean secondary energy, which plays an important role in achieving “carbon neutrality”. With the expansion of hydrogen production scale and the reduction of cost, hydrogen energy is expected to become the main body of secondary energy together with electricity [1–3]. Hydrogen production, storage, transportation, and energy conversion are the four major technical links of hydrogen energy [4–9]. Currently, more than 90% of the commercial H₂ all over the world is produced from fossil fuels through the pathways of water-gas shift reaction (WGSR) and methane steam reforming (SMR) [10, 11]. However, the produced gas usually contains impurities like N₂, CO, CH₄ and CO₂, which is difficult to meet the requirements for pharmacy, semiconductor, aerospace fuel, fuel cell and other applications. Therefore, it is necessary to separate and purify the raw H₂ product [12].

The main methods for hydrogen purification include pressure swing adsorption (PSA), cryogenic separation, membrane separation and metal hydride separation. PSA achieves hydrogen separation by using the pressure-dependent adsorption of the gas with different polarities in solid adsorbents (such as zeolites and silica gels). Under high pressure, the polarized impurity gases are adsorbed, while the non-polar hydrogen molecules

are recovered at the top of the adsorption column, achieving a high purity of 99.999%. PSA is one of the mature and popular technologies in the industry, but the hydrogen recovery is low (~ 75%). Cryogenic separation can be divided into cryogenic condensation and cryogenic adsorption, both of which take the advantage of the ultralow boiling point of hydrogen (20.38 K at 1 atm). The former condenses the low boiling point impurities into a liquid phase while the latter selectively adsorbs the impurities by adsorbents. Cryogenic separation technology is suitable for large-scale hydrogen separation with moderate purity of 99%, but its wide application is limited by the large equipment investment and high energy consumption. Metal hydride separation has a high selectivity for hydrogen by using hydrogen storage materials to adsorb H₂, possessing the advantages of high purity, simple operation, low energy consumption and low material cost. However, incomplete hydrogen release usually occurs, and the gas processing capacity is small, so it is difficult to achieve large-scale production.

Compared with the above three methods, membrane separation technology is promising and competitive due to its economy, convenience, efficiency and cleanliness, thereby being considered the next generation gas separation technology [13–17]. In the 1960s, DuPont pioneered the separation of H₂/He using polyester hollow fiber membrane. In 1990, Dalian Institute of Chemical Physics, Chinese Academy of Sciences

© The Author(s) 2022. Published by Tsinghua University Press. The articles published in this open access journal are distributed under the terms of the Creative Commons Attribution 4.0 International License (<http://creativecommons.org/licenses/by/4.0/>), which permits use, distribution and reproduction in any medium, provided the original work is properly cited.

Address correspondence to shuijianglan@buaa.edu.cn

developed polysulfone composite hollow fiber membrane, which could recover hydrogen from catalytic cracking dry gas with hydrogen content of only 40%–60%, and the recovery rate was over 85%. In recent years, hydrogen separation membrane materials have made great progress [18, 19]. By optimizing the preparation process, the performance of traditional membranes has been greatly improved. For example, Zhang et al. proposed a softness regulation strategy for rigid networks and designed 14 kinds of membranes with excellent hydrogen separation capability [20]. Recently, some new membrane materials and processing technologies have emerged, providing inspiration for the design and preparation of hydrogen separation membranes [21–23].

Representative materials, such as metal-organic frameworks (MOFs), graphene oxides and MXene nanosheets have been used for hydrogen separation [24]. According to the separation mechanisms, separation membranes can be divided into microporous membranes and dense non-porous membranes. The dense membranes based on the solution-diffusion mechanism can achieve infinite selectivity for H₂ but are limited by low gas permeance. Microporous membranes are widely used in gas separation at present because of its high porosity, defined pore structure and narrow distribution of pore sizes. High quality and high durability are crucial for the practical application of microporous membranes. However, the synthesis of structurally complete and stable membranes is currently a great challenge. To address this challenge, researchers have tried a variety of strategies, including supportive modifications, and the use of additives. In this review, we will briefly introduce the membrane separation mechanism and then elaborate on the four main types of inorganic microporous membranes used for H₂ separation. We focus on the synthesis challenges and solutions of microporous membranes.

2 Separation mechanisms

Membrane separation technology is based on differences in the dissolution and diffusion of the mixed components. The driving force for gas diffusion is the pressure drop between the feed side and permeate side of the membrane. The component that preferentially permeates the membrane is called permeate, and the other components that do not permeate the membrane are called retentate. Considering that the gas passing through the membrane is not completely ideal, there are still some retentate components that can pass through the membrane. The separation efficiency is mainly determined by two factors, namely the permeability (P) and the selectivity of the membrane. For composite membranes and asymmetric membranes, P (permeance) can be expressed as follows:

$$P(\text{permeance}) = \frac{F}{A\Delta p} \quad (1)$$

where F is the flux of permeate gas; A is the effective area of the membrane; Δp is the pressure difference between the upstream and downstream of the membrane. The unit of permeance is defined as gas permeance unit (GPU), where $1 \text{ GPU} = 10^{-6} \text{ cm}^3(\text{STP}) \cdot \text{cm}^{-2} \cdot \text{s}^{-1} \cdot \text{cmHg}^{-1} = 3.35 \times 10^{-10} \text{ mol} \cdot \text{m}^{-2} \cdot \text{s}^{-1} \cdot \text{Pa}^{-1}$. For homogeneous membranes, P (permeation coefficient) can be expressed as follows:

$$P(\text{permeation coefficient}) = \frac{Fl}{A\Delta p} \quad (2)$$

where l is the membrane thickness. Barrer is the unit of permeation coefficient (1 Barrer = $10^{-10} \text{ cm}^3(\text{STP}) \cdot \text{cm} / (\text{cm}^2 \cdot \text{s} \cdot \text{cmHg})$).

Selectivity is divided into ideal selectivity α_{AB}^* and mixed gas selectivity α_{AB}

$$\alpha_{AB}^* = \frac{P_A}{P_B} \quad (3)$$

where P_A and P_B are the permeance of gas species A and B in the membrane, respectively.

$$\alpha_{AB} = \frac{y_A / x_A}{y_B / x_B} \quad (4)$$

where y_A and y_B are the molar fractions of gas species A and B in the permeate side, while x_A and x_B are the molar fractions of gas species A and B in the feed side.

Porous membranes are grouped by the rate of gas passing through the pores of the membrane, and the separation performance is related to the type of gas and the pore size of the membrane. The transmission mechanisms of gas through porous membranes include Knudsen diffusion, surface diffusion, and molecular sieve, as shown in Fig. 1 [25]. Knudsen diffusion means that when the mean free path of gas molecules is greater than the diameter of the membrane pores, the probability of gas molecules colliding with the pore wall is much greater than the probability of gas molecules colliding with each other. The pore size for Knudsen diffusion is generally in the range of 2–100 nm. Surface diffusion means that the gas molecules are first absorbed on the membrane surface and then diffuse to the low pressure side along the pore wall. The pore size for the surface diffusion is generally less than 10 nm. Molecular sieving is suitable for gas molecules whose dynamics diameter is smaller than the pore diameter of the membrane. Only gas molecules smaller than the pore size are allowed to pass through the membrane, while other gas molecules are blocked. H₂ separation by microporous membranes mainly relies on the molecular sieving mechanism.

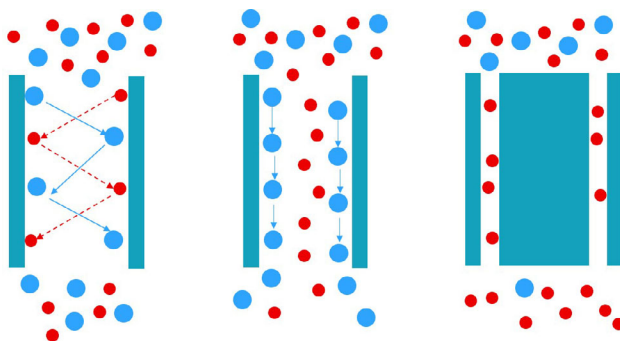


Figure 1 Schematic diagram of gas transport mechanisms in gas separation membranes.

3 Inorganic microporous membranes

According to different materials, inorganic microporous membranes for H₂ separation can be divided into zeolite membranes, silica membranes, carbon-based membranes and MOF membranes. Each microporous membrane has its unique advantages and deficiencies. For example, zeolite membranes have the characteristics of periodic topology structure, high crystallinity, regular pore shape and low cost. Whereas, their

crystalline frameworks are ready to be destroyed at conditions, such as high temperature, high water vapor pressure or acidity/basicity environments. Silica membranes have advantages in terms of ultra-micropores and facile fabrication. However, silica membranes are sensitive to steam. As typical carbon membranes, carbon molecular sieve (CMS) membranes show high permeance yet moderate separation selectivity due to the combination of ultra-micropores and micropores. MOF membranes are featured with large specific surface area, high porosity, the diverse structured [26]. The H₂ separation performances of reported microporous membranes are listed in Table 1.

3.1 Zeolite membranes

Zeolite is a type of crystal with well-defined pore structures (typically 0.3–1.0 nm), high temperature resistance and high mechanical strength, and thereby has attracted attention in gas separation. The main components of zeolite include silicate, aluminumphosphate and silicoaluminophosphate [27]. LTA, CHA, MFI, DDR, and FAU have been successfully synthesized as zeolite membranes. And zeolite membranes are usually held on porous supports such as alumina, stainless steel, titania and silica [28]. For example, ZSM-5 membranes were prepared on the support of macroporous clay for gas separation [29]. The defects, such as cracks, pinholes and intercrystalline pores,

often occur in the synthesis of zeolite membranes, which seriously affect the performance of zeolite membranes. The synthesis of defect-free zeolite membranes is still a challenge. Progresses have been made towards this target by new synthesis strategies:

(1) **Process optimization:** Synthesis method and removal of template are key steps in membrane preparation. Secondary growth is one of the most common and efficient synthesis methods. Chen et al. prepared MFI zeolite membranes on alumina hollow fibers using secondary growth and found that gas permeability of the membrane increased with the substrate curvature [30]. In addition, the secondary growth was applied to the synthesis of fluorine-free STT, Si-CHA and hydroxysodalite (H-SOD) zeolite membranes [31–33]. The traditional hydrothermal synthesis is conducted at high temperature and high pressure, causing high cost and energy consumption. To avoid these disadvantages, Sen et al. prepared LTA membranes at room temperature using sonication-assisted hydrothermal method, which could not only shorten the crystallization time, but also realize a green synthesis [34].

Most of the zeolite membranes are prepared with template agents, which are usually removed by heat-treatment before use. However, this process often leads to defects in the membrane. New methods to remove the templating agents have been developed. For example, intercrystalline defects

Table 1 Comparison of microporous membranes for H₂ separation

Membrane	Name	T (°C)	Δp (bar)	H ₂ permeance or permeability	Separation factor		
					H ₂ /N ₂	H ₂ /CO ₂	H ₂ /CH ₄
Zeolite36	FAU	100	1	4×10^{-7} mol·m ⁻² ·s ⁻¹ ·Pa ⁻¹	6	6.5	4
Zeolite43	SSZ-13	200	2	4.2×10^{-8} mol·m ⁻² ·s ⁻¹ ·Pa ⁻¹	28.4	—	263
Zeolite45	SAPO-34	250	10	3.7×10^{-7} mol·m ⁻² ·s ⁻¹ ·Pa ⁻¹	32	—	—
Zeolite34	LTA	30	1	2.2×10^{-6} mol·m ⁻² ·s ⁻¹ ·Pa ⁻¹	—	16.2	—
Zeolite41	MFI	450		1.1×10^{-7} mol·m ⁻² ·s ⁻¹ ·Pa ⁻¹	—	8.2	—
Zeolite32	Si-CHA	25	2	1.4×10^{-6} mol·m ⁻² ·s ⁻¹ ·Pa ⁻¹	—	—	85
Zeolite31	STT	25	2	2.8×10^{-8} mol·m ⁻² ·s ⁻¹ ·Pa ⁻¹	—	—	49.6
Zeolite35	DD3R	30	1	1.8×10^{-8} mol·m ⁻² ·s ⁻¹ ·Pa ⁻¹	—	—	124
Zeolite40	FAU	50	1	1.9×10^{-7} mol·m ⁻² ·s ⁻¹ ·Pa ⁻¹	—	—	9.9
Silica55	BTESE	200	2	1.8×10^{-7} mol·m ⁻² ·s ⁻¹ ·Pa ⁻¹	100	16	400
Silica51	TEOS/MTES	200	1	1.5×10^{-6} mol·m ⁻² ·s ⁻¹ ·Pa ⁻¹	18	8	—
Silica49	TEOS/TFPTES	200	1	3.1×10^{-6} mol·m ⁻² ·s ⁻¹ ·Pa ⁻¹	—	15.2	—
Silica50	TEOS/PFDTES	300	1	9.7×10^{-7} mol·m ⁻² ·s ⁻¹ ·Pa ⁻¹	—	12.1	—
Carbon61	PEK-C	30	0.1	5,260 Barrer	142	75	311
Carbon62	OrL	35	1.1	1.3×10^{-7} mol·m ⁻² ·s ⁻¹ ·Pa ⁻¹	293	—	584
Carbon59	PPO/PVP	25	2	1,121 Barrer	163.9	—	160.9
Carbon60	PI	25	2	376 Barrer	33.2	—	16.4
Carbon63	PEI	25	2	1,300 Barrer	—	—	174
Carbon66	CHFM	130	2	5×10^{-8} mol·m ⁻² ·s ⁻¹ ·Pa ⁻¹	800	83.9	5,700
MOF85	ZIF-95	325	1	1.9×10^{-6} mol·m ⁻² ·s ⁻¹ ·Pa ⁻¹	10.2	25.7	11
MOF92	ZIF-95	200	1	1.7×10^{-7} mol·m ⁻² ·s ⁻¹ ·Pa ⁻¹	36.8	41.6	40.3
MOF88	ZIF-7	30	1	2×10^{-7} mol·m ⁻² ·s ⁻¹ ·Pa ⁻¹	8.2	4.6	9.8
MOF91	ZIF-8	70	1	1.1×10^{-7} mol·m ⁻² ·s ⁻¹ ·Pa ⁻¹	9.6	8.1	13.6
MOF93	ZIF-L	30	1	2×10^{-7} mol·m ⁻² ·s ⁻¹ ·Pa ⁻¹	7.7	15.2	—
MOF89	ZIF-67	30	1	5.6×10^{-7} mol·m ⁻² ·s ⁻¹ ·Pa ⁻¹	14.7	—	15.3
MOF82	UiO-66	25	1	1.6×10^{-7} mol·m ⁻² ·s ⁻¹ ·Pa ⁻¹	—	7.3	19.6
MOF99	2D-MOF	30	1	1.7×10^{-7} mol·m ⁻² ·s ⁻¹ ·Pa ⁻¹	38.4	42.7	51.3
MOF105	2D-MOF	35	1	8.2×10^{-7} mol·m ⁻² ·s ⁻¹ ·Pa ⁻¹	—	12.6	—

appeared in DD3R zeolite membranes after an air calcination at 700 °C. Du et al. removed the template agent by a treatment in the ozone atmosphere at 473 K for 80 h and realized efficient scale-up synthesis of hollow fiber DD3R zeolite membranes [35].

(2) **Support pre-treatment:** Defects are easily generated at the interface between the film layer and the support. By modifying the support, the binding force between the membranes and the support can be improved. The decorative materials commonly used are 3-aminopropyltriethoxysilane (APTES) [36, 37], 3-chlropropylpyrimethoxysilane (CPTMS) [38], polydopamine (PDA) [39, 40], etc. Huang et al. used CPTMS as a covalent linker to strengthen the attachment of the zeolite membrane and the α -Al₂O₃ support, resulting in a dense and intact LTA membrane. A series of superior separation factors were obtained, such as 3.6 for H₂/CH₄, 4.2 for H₂/N₂, 4.4 for H₂/O₂ and 5.5 for H₂/CO₂ (Fig. 2) [37].

(3) **Membrane post-treatment:** In the preparation of zeolite membrane, post-treatments of the synthesized membrane are usually necessary to repair the defects and improve the separation performance. Zhu and Hong et al. used chemical vapor deposition (CVD) [41] and catalytic cracking deposition [42] respectively, to deposit methylidethoxysilane (MDES) in the pores of MFI membranes to reduce the pore size and increase the separation factors of H₂/CO₂. TiCl₄ and ethylene glycol (EG) were also used as precursors of the molecular layer deposition (MLD) to deposit titanium alkoxide on SSZ-13 (Fig. 3) [43]. Gao's group studied the function of 3-dimensional alkali lignin molecule on a NaA zeolite membrane and improved the selectivity of H₂ relative to the linear molecules such as N₂ and CO₂ [44]. Utilizing high selective and fast diffusion of H₂ in palladium, Jiang et al. deposited Pd on SAPO-34 membrane to increase the selectivity for H₂/N₂ mixture [45].

3.2 Silica membranes

Microporous silica membranes consist of angular-sharing tetrahedral SiO₄, which form a three-dimensional (3D) network through covalent bonds and a 0.5 nm pore size. They can separate small gas molecules such as H₂, He or O₂ [46]. Gavalas et al. [47] in 1989 and Kitao et al. [48] in 1990 synthesized silica membranes for H₂ separation by CVD and sol-gel (SG) methods, respectively. Subsequently, other research groups have prepared different types of silica membranes based on these two methods for gas separation and desalination, etc. However, silica films face the challenge of structural instability in hot and humid environments. When the surface of the membrane adsorbs steam, a condensation reaction is initiated, resulting in collapse

of the microporous structure and reduction of gas permeation flux and separation effect. The poor hydrothermal stability of silica films greatly limits their applications in the fields of WGSR and SMR. Two strategies have been reported to address this problem.

One method is improving the hydrophobicity of the film by adding hydrophobic groups [49–51]. De Vos et al. modified the silica membrane using methyl group and the hydrophobicity was increased by 10 times [52]. The other method is the introduction of metal or metal oxide, such as Pd [53], Co [54], and Zr [55]. Doping is generally conducted in two ways. One way is to generate Si-O-X bonds (X is a doping element), which are structurally more stable than Si-O-Si bonds, so it can improve the resistance of the membranes to the humidity environment. Boffa et al. demonstrated that the hydrogen permeance of the Nb-doped membranes declined by 32% after a hydrothermal treatment at 200 °C, while that of the silica membranes declined by 73% [56]. Another way is to disperse metal or metal oxide in the network of the silica film, which plays a role of support or the skeleton structure of the membrane. Kanezashi et al. fabricated Ni-doped silica membranes, which exhibited high H₂ permeance of 4.6×10^{-6} m³(STP)·m⁻²·s⁻¹·kPa⁻¹ and ideal selectivity of 400 in the separation of H₂/N₂ even after exposure to steam at 500 °C for one week [57].

3.3 Carbon membranes

CMS membranes are prepared by high-temperature pyrolysis of polymer precursors. The disordered accumulation of aromatic carbon layers forms graphitized carbon microcrystalline structures. The gaps between the carbon layers in the crystallite structure form ultra-micropore (< 0.6 nm), and the disordered stacking of carbon crystallites forms micropores of larger sizes (0.6–2 nm). The former plays a role in molecular sieve separation, while the latter is for permeation [58]. Compared with the industrialized zeolite membrane, the pores of CMS membranes are slit-shaped, which ensures selectivity and higher gas permeability

The gas separation performance of CMS membranes is affected by pore size distribution and critical ultrafine pores, which is related to the structure of polymer precursor [59–61]. The performance could be improved by pretreatment of precursor membrane such as iron additives [62]. There are two kinds of CMS membranes: supported and unsupported membranes. To improve mechanical strength, most CMS membranes were prepared on porous substrates (e.g., alumina, ceramic, and stainless steel). Defects in CMS membranes

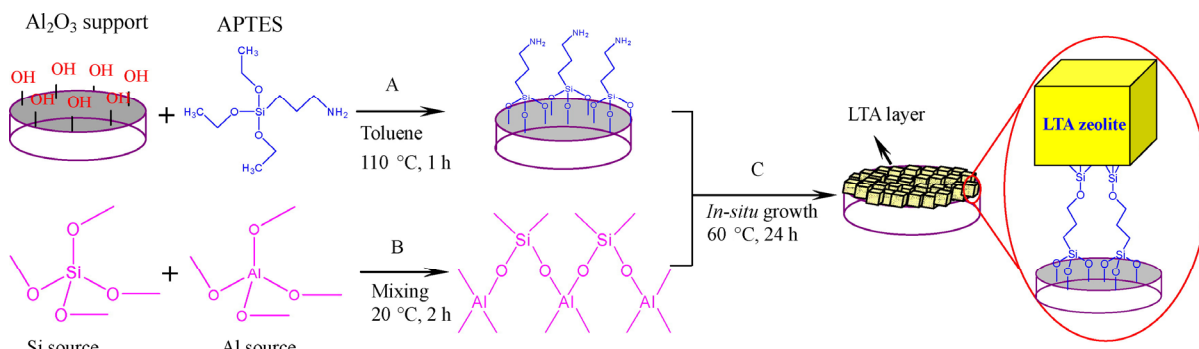


Figure 2 Schematic diagram for preparation of LTA membrane using APTES as a covalent linker between LTA zeolite membrane and alumina support. Reproduced with permission from Ref. [37], © Elsevier B. V. 2009.

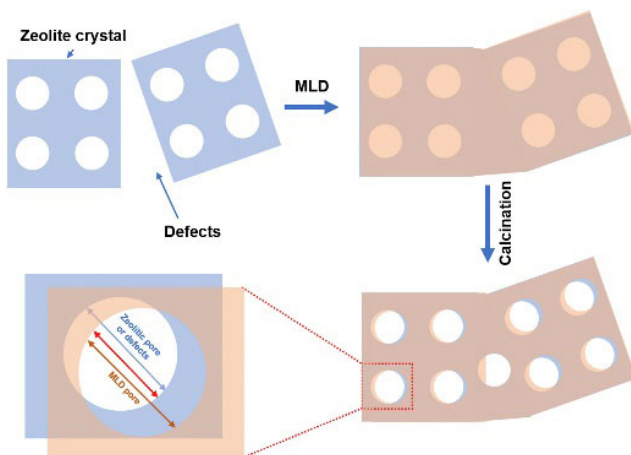


Figure 3 Schematic illustration of surface crystal pore mouth reduction by pore misalignment and defects flow restriction via MLD on polycrystalline zeolite membrane. Reproduced with permission from Ref. [43], © Elsevier B. V. 2021.

may be caused by tough surface of the substrate and great difference in thermal expansion between the substrate and the precursor membrane. Therefore, membrane performances could be improved by optimizing the support through high-temperature sintering [63], polishing and interfacial interaction modification [64]. Li et al. improved the smoothness of the $\alpha\text{-Al}_2\text{O}_3$ support by adding TiO_2 and grinding/polishing, which showed good adhesion to the deposited polymer. On the other hand, the TiO_2 modification narrowed the thermal expansion coefficient gap between the substrate and the polymer film, resulting in a defect-free tubular carbon film (Fig. 4) [65].

As typical unsupported CMS membrane, CMS hollow fibers show high packing density and excellent separation performance. However, these membranes face the challenge of pore collapse during carbonization and physical aging. For the first problem, when asymmetric cellulose hollow fiber was used as the precursor, direct drying of water-filled cellulose membranes would cause the pore collapse. Lei et al. developed a drying method to maintain the pore structure by exchanging non-solvent (water-isopropanol-n-hexane) [66]. For the

physical aging, Qiu et al. performed post-pyrolysis hyperaging treatment from 90 to 200 °C. This treatment led to the smaller ultra-micropore and improved $\text{H}_2/\text{C}_2\text{H}_4$ selectivity while maintaining high H_2 permeance [67].

As a new type of carbon-based membrane, graphene-based membranes received much attention. Graphene is a periodic hexagonal honeycomb crystal made up of sp^2 hybrid carbon atoms. Theoretically, graphene cannot permeate gas molecules or even helium molecules [68], because the π orbital of graphene produces a huge electron cloud, which blocks the pores of aromatic rings. To achieve gas permeability, graphene membranes can be drilled through oxidation etching and electron bombardment. Steven et al. [69] used the ultraviolet (UV)-induced oxidation etching method to introduce holes on the graphene surface, and obtained a H_2 leak rate of $4.5 \times 10^{-23} \text{ mol}\cdot\text{s}^{-1}\cdot\text{Pa}^{-1}$ (Fig. 5). However, an economical and efficient way to drill holes in large-area graphene remains a challenge [70]. To circumvent this problem, researchers turned their attention to assembled graphene oxide (GO) membranes.

Due to the two-dimensional (2D) sheet structure, GOs are easy to stack and then form assembled GO membranes. Unique 2D channels are formed between the layers for gas diffusion. There are many ways to assemble GO nanosheets. Using vacuum/pressure-assisted filtration devices to assemble GO nanosheets is the simplest method and could easily control the thickness of the film. For other methods, such as spin coating [71, 72] and spraying, the construction of self-assembled GO membranes relies on the attraction between the spinning surfaces and the inherent repulsive force at the edges of graphene sheets. Shen et al. used outer force and inner force to overcome the electrostatic force between GO nanosheets and improved the order degree of self-assembly of GO membranes with H_2 permeability of 840–1,200 Barrer and H_2/CO_2 selectivity of 29–33 at 0.2 MPa and 25 °C (Fig. 6) [73]. The hybridization of membranes is also a way to adjust selectivity. For example, ZIF-8 particles were intergrown into GO membranes, which lead to high H_2 selectivity relative to CO_2 , N_2 and CH_4 [74].

3.4 MOF membranes

MOFs are constructed by metal cluster as a secondary structural unit connected to the organic ligand by chemical

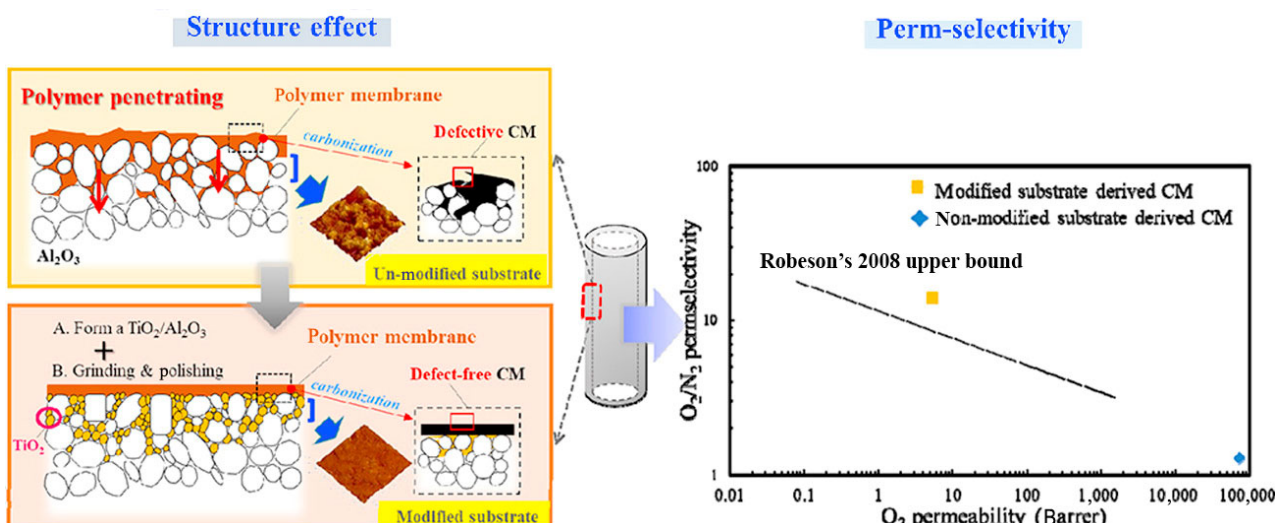


Figure 4 Schematic diagram of the difference between conventional CMS membranes and TiO_2 modified CMS membranes. Reproduced with permission from Ref. [65], © Hydrogen Energy Publications LLC 2019.

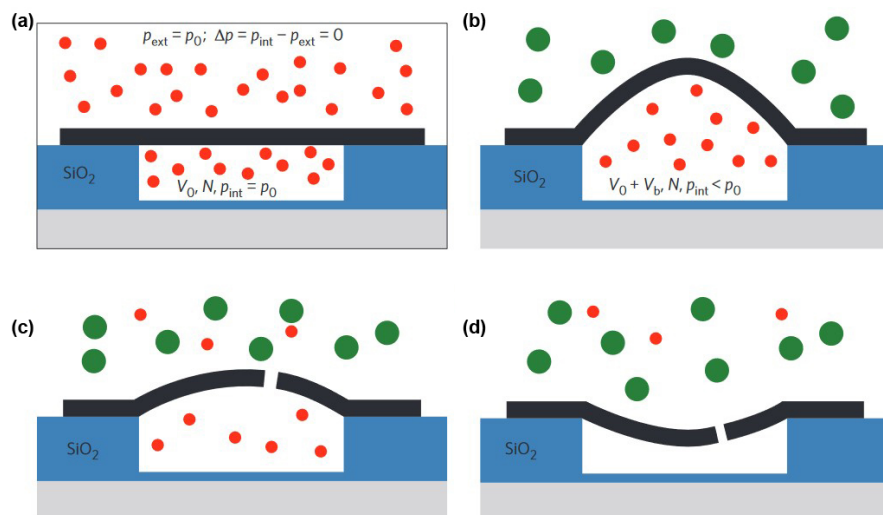


Figure 5 Schematics of a microscopic graphene membrane on a silicon oxide substrate: (a) pristine graphene fabricated by exfoliation; (b) bulge upwards of the membrane after removing the graphene membrane from the pressure chamber; (c) H₂ leaking out of the microchamber through the etching pores; (d) deflecting downwards of the membrane after all H₂ molecules leaking out. Reproduced with permission from Ref. [69], © Nature Publishing Group 2012.

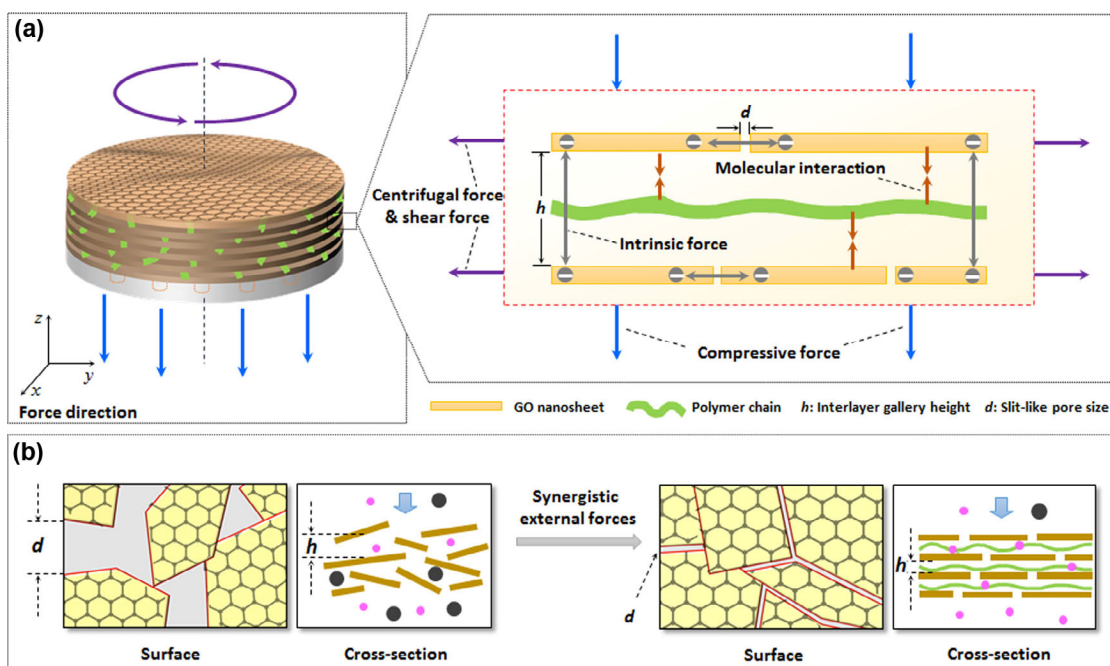


Figure 6 Design and construction of 2D channels. (a) External force driven assembly approach for fabricating 2D channels. (b) Hypothetical evolution of surface and cross section of GO-assembled 2D channels from intrinsic force induced disordered structure (left) to highly ordered laminar structures (right) driven by introduced synergistic external force. Reproduced with permission from Ref. [73], © American Chemical Society 2016.

bonds, which have characteristics of ordered open channels (0.3–0.9 nm), diversified structures, large specific surface area and adjustable chemical environment [75]. Many attempts have been made to adjust the pore size and properties of MOF to find suitable MOF membranes for separating gas mixtures. Various MOF membranes have been prepared for gas or liquid separation, such as MOF-5 [76], Cu₃(BTC)₂ [77], ZIF-8 [78, 79], ZIF-90 [80], MIL-160 [81], UiO-66-NH₂ [82] membranes. The continuity of MOF membranes is the basis for the gas separation. At present, how to effectively regulate the growth of crystals to prepare membranes with complete and dense structure and close combination with supports is the biggest challenge. To address this challenge, several synthetic strategies have been developed:

(1) In-situ growth: After placing the support in the reaction solution, a large number of crystals nucleate on the carrier and grow into thin films under appropriate supersaturation conditions by *in-situ* synthesis. The morphology of the synthesized MOF membranes was controlled by the concentration of reactants, and the reaction temperature and duration [78, 83, 84]. In 2009, Liu et al. prepared a MOF-5 membrane on a α-alumina support and Bux et al. obtained a ZIF-8 membrane on a titania support by *in-situ* solvothermal synthesis [76, 78]. It should be noted that this method is very sensitive to the synthesis conditions and the chemical and physical properties of the porous supports.

Modifying the support surface by coupling agents can introduce functional groups that can coordinate with MOF

crystals by chemical bonding. As such, the heterogeneous nucleation density of MOF crystals and the bonding force between the support and the MOF membranes are significantly increased, and thereby the repeatability of MOF films is improved. Commonly used coupling agents are APTES, PDA, and polyaniline (PAN) [85–87]. Huang et al. prepared a series of MOF membranes including ZIF-8, ZIF-22, ZIF-7, ZIF-95 and ZIF-90 membranes using APTES modification. The coordination sites offered by the amine group in APTES could anchor the free Zn^{2+} in the reaction system, thus enhancing the interfacial bonding strength and providing more nucleation sites at the same time.

The support can also be modified by inorganic materials such as metal oxides and metal hydroxides, which provide metal sources for the nucleation and growth of MOFs. Zhang et al. prepared ZIF-8 and ZIF-67 films using homologous metal oxide as inducing layers by *in-situ* growth [88, 89]. In addition, the atomic layer deposition (ALD) was used to achieve metal transition layers [90]. Zhou et al. deposited ZnO , $Co(OH)_2$, and Cu_2O coatings on stainless steel mesh by electrodeposition method, and obtained ZIF-8, ZIF-67 and HKUST-1 membranes respectively after conversion of ligand solution (Fig. 7) [91].

(2) **Secondary growth:** The secondary growth method refers to pre-introducing MOF grains as a seed layer on the surface of the support to improve heterogeneous nucleation sites. Compared with the *in-situ* crystallization method, the secondary growth method effectively overcomes the problem of low nucleation density on the surface of the support.

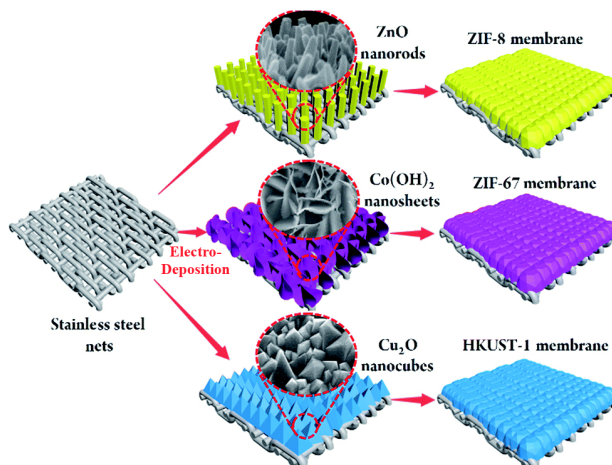


Figure 7 Schematic illustration of the *in-situ* growth of three different MOF membranes on supports modified by electrodeposition. Reproduced with permission from Ref. [91], © Royal Society of Chemistry 2017.

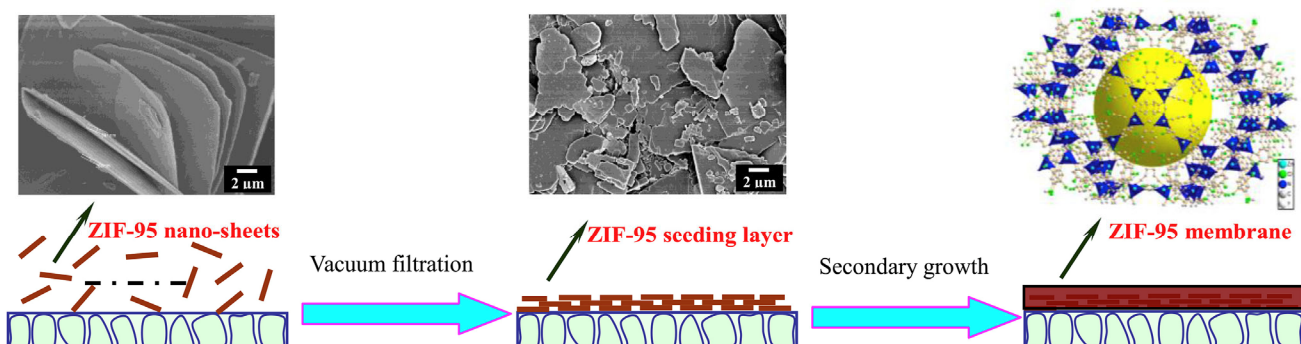


Figure 8 Scheme of the synthesis of ZIF-95 membranes through secondary growth method using ZIF-95 nano-sheets as seeds. Reproduced with permission from Ref. [92], © Elsevier B. V. 2019.

Moreover, the nucleation and growth processes can be separated by introducing a seed layer in advance to better control the MOF grain size, film thickness and film orientation. Ma et al. coated ZIF-95 nano-sheets as a seeding layer by vacuum filtration and then obtained a well-intergrown ZIF-95 membrane, which exhibited H_2 permeances of $1.7 \times 10^{-7} \text{ mol}\cdot\text{m}^{-2}\cdot\text{s}^{-1}\cdot\text{Pa}^{-1}$ and separation factors of 41.6, 36.8, and 40.3 for H_2/CO_2 , H_2/N_2 , and H_2/CH_4 respectively (Fig. 8) [92]. Chemical modification is also used in the secondary growth. ZIF-8 and MOF-5 films were synthesized on polyethylenimine (PEI) modified support by secondary growth method, which improved the adhesion between the MOF seed layer and the support [93, 94]. PEI can also be used to modify the seeds to increase the number of active functional groups on the surface of the seed crystal and the viscosity of the seed crystal solution.

(3) **Contra-diffusion:** The interfacial reverse diffusion method utilizes a porous support to separate the ligand solution and the metal source solution (Fig. 9) [95, 96]. Driven by the concentration difference, the ligands and metal sources will preferentially diffuse to the interface and nucleate at the interface to form dense and continuous MOF films. Yao et al. prepared ZIF-8 membranes on the surface of nylon substrate by contra-diffusion method. Due to the different diffusion rates of Zn^{2+} and 2-methylimidazole on two sides of the support, ZIF-8 grains preferentially grew on the Zn^{2+} side. At the same time, ZIF-8 crystals partially grew in the pores of the nylon support, which enhanced the interaction between the membrane layer and the support [97].

(4) **Vapor phase transformation:** Metal sources are deposited on the surface of porous support in advance, and then the gas-phase ligands are introduced to the support to transform the metal sources into MOF membranes. Vapor phase transformation could control the thickness of MOF film by changing the content of depositions. Stassen et al. reported a series of ZIF-8 films with controllable thickness by chemical vapor deposition. First, the ZnO metal source was uniformly coated on the surface of a porous support of silicon dioxide by ALD, and then it was transformed into ZIF-8 film by the reaction with 2-methylimidazole vapor [98]. Considering the difficulty of the scale-up of ALD, Li et al. developed the gel-vapor deposition (GVD) method, which effectively combined the Zn sol-gel coating and the ligand vapor deposition for environmentally friendly synthesis [12]. Likewise, Zhang et al. prepared a two-dimensional Co-based membrane with high H_2/CO_2 separation performance by the vapor phase transformation method. As illustrated in Fig. 10, a Co-based gel was first dip-coated on the outer surface of a ceramic tube, and then

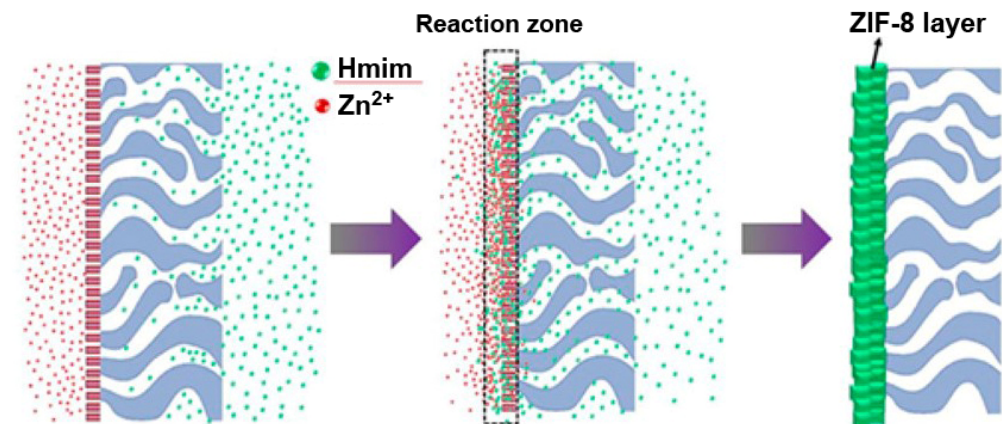


Figure 9 Schematic diagram of the preparation of ZIF-8 membrane using contra-diffusion synthesis. Reproduced with permission from Ref. [95], © American Chemical Society 2016.

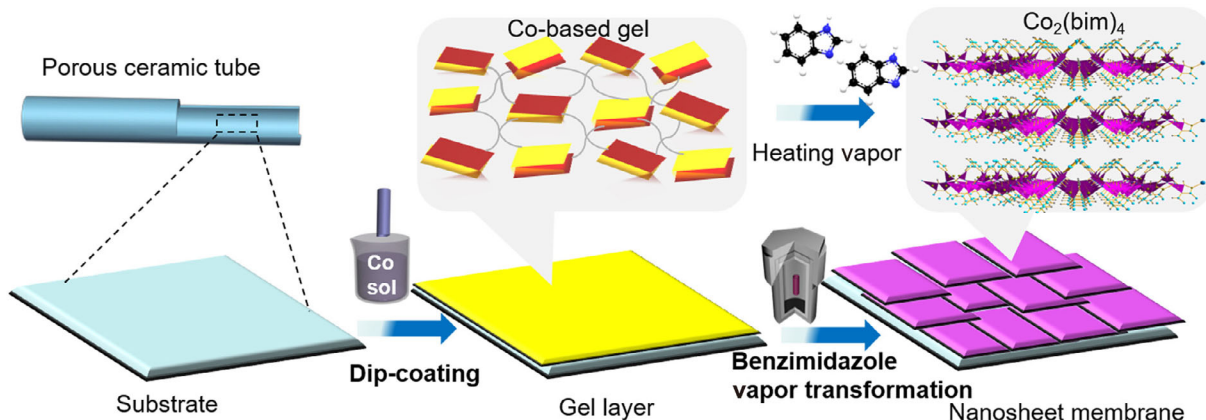


Figure 10 Schematic diagram of two-dimensional Co-based zeolitic imidazolate framework nanosheet membrane produced via vapor phase transformation of Co-based gel. Reproduced with permission from Ref. [99], © Elsevier B. V. 2018.

the highly oriented Co-based MOF membrane was prepared after the solvent-free vapor phase transformation. The Co-based gel played multiple roles including providing metal sources, guiding the growth direction of nanosheet films and controlling the film thickness [99].

Moreover, fast current-driven synthesis [100, 101], microfluidic channel-embedded solution-shearing [102], supercritical fluids assistance [103] are newly emerging strategies for framework design or scaled-up manufacturing of MOF membranes.

In addition to the bulk MOF membranes, ultrathin 2D MOF nanosheets that can minimize transport resistance are innovative membrane materials for H₂ separation. Peng et al. exfoliated poly(Zn₂(benzimidazole)₄) (Zn₂(bim)₄) molecular sieve nanosheets (MSNs) by a soft-physical process, which were coated on α -Al₂O₃ to obtain MSN membranes with H₂ permeance of 760 to 3,760 GPU and H₂/CO₂ selectivity of 53 to 291 at room temperature and 1 atm [104]. As illustrated in Fig. 12, Ma et al. designed thin-film composite membranes combining microporous polyacrylate and 2D MOF nanosheets, which provided a new scheme for the structure design of separation membranes [105].

4 Conclusion and outlook

In recent years, a variety of new synthetic methods have been used to prepare microporous membranes for hydrogen

separation. Zeolite membranes are a type of separation membranes with the longest research history, and they face severe challenges of efficient and defect-free synthesis. The solutions mainly include process optimization, support pre-treatment and membrane post-treatment. For silica membranes, the stability can be improved by introducing hydrophobic groups and metal elements. For carbon molecular sieve membranes, support pretreatment and process optimization are the main improvement methods for polymer-based membranes; while graphene oxide membranes provide new opportunities for carbon molecular sieves. MOF membrane is an emerging porous membrane material, and its main synthesis methods include *in situ* growth, secondary growth, contra-diffusion and vapor phase transformation.

With the advancement of materials science, new materials and advanced processing technologies continue to emerge, which will surely enrich the family of microporous membranes and enhance their gas separation capabilities. Porous membranes made of two-dimensional materials represented by GO have the advantages of low transport resistance and large permeation flux, and meanwhile, their gas transport channels and pore sizes can be precisely controlled in the sub-nanometer size range [106, 107]. Therefore, 2D materials have great promise in preparing microporous membranes for hydrogen separation. In addition, it is worth noting that some Mg-based MOFs have recently been reported to exhibit room-temperature hydrogen storage capability. The hydrogen separation membranes

made of such MOFs with hydrogen storage capacity will change the gas separation mechanism and are expected to improve the purity of the hydrogen product.

Acknowledgements

This work was supported by the National Key Research and Development Program of China (No. 2021YFB4000601), the National Natural Science Foundation of China (Nos. 21975010, U21A20328, and 51731002), and the Natural Science Foundation of Beijing Municipality (No. Z200012).

Declaration of conflicting interests

The authors declare no conflicting interests regarding the content of this article.

References

- [1] Shih, A. J.; Haile, S. M. Electrifying membranes to deliver hydrogen. *Science* **2022**, *376*, 348–349.
- [2] Guo, X.; Wan, X.; Liu, Q. T.; Li, Y. C.; Li, W. W.; Shui, J. L. Phosphated IrMo bimetallic cluster for efficient hydrogen evolution reaction. *eScience*, in press, DOI: 10.1016/j.esci.2022.04.002.
- [3] Han, Q.; Wang, B.; Gao, J.; Qu, L. T. Graphitic carbon nitride/nitrogen-rich carbon nanofibers: Highly efficient photocatalytic hydrogen evolution without cocatalysts. *Angew. Chem., Int. Ed.* **2016**, *55*, 10849–10853.
- [4] Liu, S. Y.; Liu, J. Y.; Liu, X. F.; Shang, J. X.; Xu, L.; Yu, R. H.; Shui, J. L. Hydrogen storage in incompletely etched multilayer Ti₂CT_x at room temperature. *Nat. Nanotechnol.* **2021**, *16*, 331–336.
- [5] Liu, Q. T.; Li, Y. C.; Zheng, L. R.; Shang, J. X.; Liu, X. F.; Yu, R. H.; Shui, J. L. Sequential synthesis and active-site coordination principle of precious metal single-atom catalysts for oxygen reduction reaction and PEM fuel cells. *Adv. Energy Mater.* **2020**, *10*, 2000689.
- [6] Yang, C. L.; Wang, L. N.; Yin, P.; Liu, J. Y.; Chen, M. X.; Yan, Q. Q.; Wang, Z. S.; Xu, S. L.; Chu, S. Q.; Cui, C. H. et al. Sulfur-anchoring synthesis of platinum intermetallic nanoparticle catalysts for fuel cells. *Science* **2021**, *374*, 459–464.
- [7] Liu, J. Y.; Wan, X.; Liu, S. Y.; Liu, X. F.; Zheng, L. R.; Yu, R. H.; Shui, J. L. Hydrogen passivation of M-N-C (M = Fe, Co) catalysts for storage stability and ORR activity improvements. *Adv. Mater.* **2021**, *33*, 2103600.
- [8] Chen, M.; Pu, Y. H.; Li, Z. Y.; Huang, G.; Liu, X. F.; Lu, Y.; Tang, W. K.; Xu, L.; Liu, S. Y.; Yu, R. H. et al. Synergy between metallic components of MoNi alloy for catalyzing highly efficient hydrogen storage of MgH₂. *Nano Res.* **2020**, *13*, 2063–2071.
- [9] Wang, Y. N.; Wan, X.; Liu, J. Y.; Li, W. W.; Li, Y. C.; Guo, X.; Liu, X. F.; Shang, J. X.; Shui, J. L. Catalysis stability enhancement of Fe/Co dual-atom site via phosphorus coordination for proton exchange membrane fuel cell. *Nano Res.* **2022**, *15*, 3082–3089.
- [10] Kajama, M. N.; Nwogu, N. C.; Gobina, E. Preparation and characterization of inorganic membranes for hydrogen separation. *Int. J. Hydrot. Energy* **2016**, *41*, 8221–8227.
- [11] Clark, D.; Malerød-Fjeld, H.; Budd, M.; Yuste-Tirados, I.; Beeaff, D.; Aamodt, S.; Nguyen, K.; Ansaloni, L.; Peters, T.; Vestre, P. K. et al. Single-step hydrogen production from NH₃, CH₄, and biogas in stacked proton ceramic reactors. *Science* **2022**, *376*, 390–393.
- [12] Li, W. B.; Su, P. C.; Li, Z. J.; Xu, Z. H.; Wang, F.; Ou, H. S.; Zhang, J. H.; Zhang, G. L.; Zeng, E. Ultrathin metal-organic framework membrane production by gel-vapour deposition. *Nat. Commun.* **2017**, *8*, 406.
- [13] Chuah, C. Y.; Lee, J.; Bae, T. H. Graphene-based membranes for H₂ separation: Recent progress and future perspective. *Membranes* **2020**, *10*, 336.
- [14] Shu, L.; Peng, Y.; Yao, R.; Song, H. L.; Zhu, C. Y.; Yang, W. S. Flexible soft-solid metal-organic framework composite membranes for H₂/CO₂ separation. *Angew. Chem., Int. Ed.* **2022**, *134*, e202117577.
- [15] Zhu, B.; Jiang, X.; He, S. S.; Yang, X. B.; Long, J.; Zhang, Y. Q.; Shao, L. Rational design of poly(ethylene oxide)-based membranes for sustainable CO₂ capture. *J. Mater. Chem. A* **2020**, *8*, 24233–24252.
- [16] He, S. S.; Zhu, B.; Jiang, X.; Han, G.; Li, S. W.; Lau, C. H.; Wu, Y. D.; Zhang, Y. Q.; Shao, L. Symbiosis-inspired *de novo* synthesis of ultrahigh MOF growth mixed matrix membranes for sustainable carbon capture. *Proc. Natl. Acad. Sci. USA* **2022**, *119*, e2114964119.
- [17] He, S. S.; Zhu, B.; Li, S. W.; Zhang, Y. Q.; Jiang, X.; Lau, C. H.; Shao, L. Recent progress in PIM-1 based membranes for sustainable CO₂ separations: Polymer structure manipulation and mixed matrix membrane design. *Sep. Purif. Technol.* **2022**, *284*, 120277.
- [18] Zhang, K.; Way, J. D. Palladium-copper membranes for hydrogen separation. *Sep. Purif. Technol.* **2017**, *186*, 39–44.
- [19] Lim, D. W.; Ha, J. S.; Oruganti, Y.; Moon, H. R. Hydrogen separation and purification with MOF-based materials. *Mater. Chem. Front.* **2021**, *5*, 4022–4041.
- [20] Zhang, M. X.; Jing, X. C.; Zhao, S.; Shao, P. P.; Zhang, Y. Y.; Yuan, S.; Li, Y. S.; Gu, C.; Wang, X. Q.; Ye, Y. C. et al. Electropolymerization of molecular-sieving polythiophene membranes for H₂ separation. *Angew. Chem., Int. Ed.* **2019**, *58*, 8768–8772.
- [21] Lai, H. W. H.; Benedetti, F. M.; Ahn, J. M.; Robinson, A. M.; Wang, Y. G.; Pinna, I.; Smith, Z. P.; Xia, Y. Hydrocarbon ladder polymers with ultrahigh permselectivity for membrane gas separations. *Science* **2022**, *375*, 1390–1392.
- [22] Huang, G. J.; Ghalei, B.; Isfahani, A. P.; Karahan, H. E.; Terada, D.; Qin, D. T.; Li, C. E.; Tsujimoto, M.; Yamaguchi, D.; Sugimoto, K. et al. Overcoming humidity-induced swelling of graphene oxide-based hydrogen membranes using charge-compensating nanodiamonds. *Nat. Energy* **2021**, *6*, 1176–1187.
- [23] He, S. S.; Jiang, X.; Li, S. W.; Ran, F. T.; Long, J.; Shao, L. Intermediate thermal manipulation of polymers of intrinsic microporous (PIMs) membranes for gas separations. *AIChE J.* **2020**, *66*, e16543.
- [24] Shen, J.; Liu, G. Z.; Ji, Y. F.; Liu, Q.; Cheng, L.; Guan, K. C.; Zhang, M. C.; Liu, G. P.; Xiong, J.; Yang, J. et al. 2D MXene nanofilms with tunable gas transport channels. *Adv. Funct. Mater.* **2018**, *28*, 1801511.
- [25] Li, P. Y.; Wang, Z.; Qiao, Z. H.; Liu, Y. N.; Cao, X. C.; Li, W.; Wang, J. X.; Wang, S. C. Recent developments in membranes for efficient hydrogen purification. *J. Membr. Sci.* **2015**, *495*, 130–168.
- [26] Dou, H. Z.; Xu, M.; Wang, B. Y.; Zhang, Z.; Wen, G. B.; Zheng, Y.; Luo, D.; Zhao, L.; Yu, A. P.; Zhang, L. H. et al. Microporous framework membranes for precise molecule/ion separations. *Chem. Soc. Rev.* **2021**, *50*, 986–1029.
- [27] Gascon, J.; Kapteijn, F.; Zornoza, B.; Sebastián, V.; Casado, C.; Coronas, J. Practical approach to zeolitic membranes and coatings: State of the art, opportunities, barriers, and future perspectives. *Chem. Mater.* **2012**, *24*, 2829–2844.
- [28] Algieri, C.; Drioli, E. Zeolite membranes: Synthesis and applications. *Sep. Purif. Technol.* **2021**, *278*, 119295.
- [29] Geus, E. R.; den Exter, M. J.; Bekkum, H. V. Synthesis and characterization of zeolite (MFI) membranes on porous ceramic supports. *J. Chem. Soc., Faraday Trans.* **1992**, *88*, 3101–3109.
- [30] Chen, C. H.; Meng, L.; Tung, K. L.; Lin, Y. S. Effect of substrate curvature on microstructure and gas permeability of hollow fiber MFI zeolite membranes. *AIChE J.* **2018**, *64*, 3419–3428.
- [31] Zhou, T.; Shi, M. Y.; Chen, L. J.; Gong, C.; Zhang, P.; Xie, J. X.; Wang, X. R.; Gu, X. H. Fluorine-free synthesis of all-silica STT zeolite membranes for H₂/CH₄ separation. *Chem. Eng. J.* **2022**, *433*, 133567.
- [32] Wu, T. Y.; Shu, C. J.; Liu, S.; Xu, B. S.; Zhong, S. L.; Zhou, R. F. Separation performance of Si-CHA zeolite membrane for a binary H₂/CH₄ mixture and ternary and quaternary mixtures containing impurities. *Energy Fuels* **2020**, *34*, 11650–11659.

- [33] Arepalli, D.; Rehman, A. U.; Kim, M. Z.; Alam, S. F.; Cho, C. H. Optimal synthesis of nanosize seeds for secondary growth of high performance hydroxy-sodalite (H-SOD) zeolite membranes for small gas and water separations. *Microporous Mesoporous Mater.* **2022**, *329*, 111451.
- [34] Sen, M.; Dana, K.; Das, N. Development of LTA zeolite membrane from clay by sonication assisted method at room temperature for H₂-CO₂ and CO₂-CH₄ separation. *Ultrason. Sonochem.* **2018**, *48*, 299–310.
- [35] Du, P.; Song, J. Y.; Wang, X. R.; Zhang, Y. T.; Xie, J. X.; Liu, G.; Liu, Y. L.; Wang, Z. W.; Hong, Z.; Gu, X. H. Efficient scale-up synthesis and hydrogen separation of hollow fiber DD3R zeolite membranes. *J. Membr. Sci.* **2021**, *636*, 119546.
- [36] Huang, A. S.; Wang, N. Y.; Caro, J. Seeding-free synthesis of dense zeolite FAU membranes on 3-aminopropyltriethoxysilane-functionalized alumina supports. *J. Membr. Sci.* **2012**, *389*, 272–279.
- [37] Huang, A. S.; Liang, F. Y.; Steinbach, F.; Caro, J. Preparation and separation properties of LTA membranes by using 3-aminopropyltriethoxysilane as covalent linker. *J. Membr. Sci.* **2010**, *350*, 5–9.
- [38] Huang, A. S.; Liu, Q.; Wang, N. Y.; Tong, X.; Huang, B. X.; Wang, M.; Caro, J. Covalent synthesis of dense zeolite LTA membranes on various 3-chloropropyltrimethoxysilane functionalized supports. *J. Membr. Sci.* **2013**, *437*, 57–64.
- [39] Zhu, F.; Landon, J.; Liu, K. L. FAU zeolite membranes for dewatering of amine-based post-combustion CO₂ capture solutions. *AIChE J.* **2020**, *66*, e17042.
- [40] Zhou, C.; Yuan, C. F.; Zhu, Y. Q.; Caro, J.; Huang, A. S. Facile synthesis of zeolite FAU molecular sieve membranes on bio-adhesive polydopamine modified Al₂O₃ tubes. *J. Membr. Sci.* **2015**, *494*, 174–181.
- [41] Zhu, X. F.; Wang, H. B.; Lin, Y. S. Effect of the membrane quality on gas permeation and chemical vapor deposition modification of MFI-type zeolite membranes. *Ind. Eng. Chem. Res.* **2010**, *49*, 10026–10033.
- [42] Hong, Z.; Sun, F.; Chen, D. D.; Zhang, C.; Gu, X. H.; Xu, N. P. Improvement of hydrogen-separating performance by on-stream catalytic cracking of silane over hollow fiber MFI zeolite membrane. *Int. J. Hydrol. Energy* **2013**, *38*, 8409–8414.
- [43] Dong, Q. B.; Jiang, J.; Li, S. G.; Yu, M. Molecular layer deposition (MLD) modified SSZ-13 membrane for greatly enhanced H₂ separation. *J. Membr. Sci.* **2021**, *622*, 119040.
- [44] Gao, X. C.; Da, C.; Chen, C.; Li, Z. H.; Gu, X. H.; Bhatia, S. K. The induced orientation effect of linear gases during transport in a NaA zeolite membrane modified by alkali lignin. *J. Membr. Sci.* **2021**, *620*, 118971.
- [45] Jiang, J.; Islam, S.; Dong, Q. B.; Zhou, F. L.; Li, S. G.; Yu, M. Deposition of an ultrathin palladium (Pd) coating on SAPO-34 membranes for enhanced H₂/N₂ separation. *Int. J. Hydrol. Energy* **2020**, *45*, 33648–33656.
- [46] Cardoso, S. P.; Azenha, I. S.; Lin, Z.; Portugal, I.; Rodrigues, A. E.; Silva, C. M. Inorganic membranes for hydrogen separation. *Sep. Purif. Technol.* **2018**, *47*, 229–266.
- [47] Gavalas, G. R.; Megiris, C. E.; Nam, S. W. Deposition of H₂-permselective SiO₂ films. *Chem. Eng. Sci.* **1989**, *44*, 1829–1835.
- [48] Kitao, S.; Kameda, H.; Asaeda, M. Gas separation by thin porous silica membrane of ultra fine pores at high temperature. *Membrane* **1990**, *15*, 222–227.
- [49] Wei, Q.; Wang, F.; Nie, Z. R.; Song, C. L.; Wang, Y. L.; Li, Q. Y. Highly hydrothermally stable microporous silica membranes for hydrogen separation. *J. Phys. Chem. B* **2008**, *112*, 9354–9359.
- [50] Wei, Q.; Ding, Y. L.; Nie, Z. R.; Liu, X. G.; Li, Q. Y. Wettability, pore structure and performance of perfluorodecyl-modified silica membranes. *J. Membr. Sci.* **2014**, *466*, 114–122.
- [51] Giessler, S.; Jordan, L.; da Costa, J. C. D.; Lu, G. Q. Performance of hydrophobic and hydrophilic silica membrane reactors for the water gas shift reaction. *Sep. Purif. Technol.* **2003**, *32*, 255–264.
- [52] de Vos, R. M.; Maier, W. F.; Verweij, H. Hydrophobic silica membranes for gas separation. *J. Membr. Sci.* **1999**, *158*, 277–288.
- [53] Kanezashi, M.; Sano, M.; Yoshioka, T.; Tsuru, T. Extremely thin Pd-silica mixed-matrix membranes with nano-dispersion for improved hydrogen permeability. *Chem. Commun.* **2010**, *46*, 6171–6173.
- [54] Igi, R.; Yoshioka, T.; Ikuhara, Y. H.; Iwamoto, Y.; Tsuru, T. Characterization of Co-doped silica for improved hydrothermal stability and application to hydrogen separation membranes at high temperatures. *J. Am. Ceram. Soc.* **2008**, *91*, 2975–2981.
- [55] ten Hove, M.; Nijmeijer, A.; Winnubst, L. Facile synthesis of zirconia doped hybrid organic inorganic silica membranes. *Sep. Purif. Technol.* **2015**, *147*, 372–378.
- [56] Boffa, V.; Blank, D. H. A.; ten Elshof, J. E. Hydrothermal stability of microporous silica and niobia-silica membranes. *J. Membr. Sci.* **2008**, *319*, 256–263.
- [57] Kanezashi, M.; Asaeda, M. Hydrogen permeation characteristics and stability of Ni-doped silica membranes in steam at high temperature. *J. Membr. Sci.* **2006**, *271*, 86–93.
- [58] Liu, J. Q.; Goss, J.; Calverley, T.; Meyers, G.; Thorseth, M. A.; Todd, C. S.; Kang, J.; Denise, A.; Clements, H.; Klann, J. et al. Self-standing permselective CMS membrane from melt extruded PVDC. *J. Membr. Sci.* **2020**, *615*, 118554.
- [59] Itta, A. K.; Tseng, H. H.; Wey, M. Y. Fabrication and characterization of PPO/PVP blend carbon molecular sieve membranes for H₂/N₂ and H₂/CH₄ separation. *J. Membr. Sci.* **2011**, *372*, 387–395.
- [60] Itta, A. K.; Tseng, H. H. Hydrogen separation performance of CMS membranes derived from the imide-functional group of two similar types of precursors. *Int. J. Hydrol. Energy* **2011**, *36*, 8645–8657.
- [61] Xu, R. S.; He, L.; Li, L.; Hou, M. J.; Wang, Y. Z.; Zhang, B. S.; Liang, C. H.; Wang, T. H. Ultraselective carbon molecular sieve membrane for hydrogen purification. *J. Energy Chem.* **2020**, *50*, 16–24.
- [62] Kumakiri, I.; Tamura, K.; Sasaki, Y.; Tanaka, K.; Kita, H. Influence of iron additive on the hydrogen separation properties of carbon molecular sieve membranes. *Ind. Eng. Chem. Res.* **2018**, *57*, 5370–5377.
- [63] Wey, M. Y.; Tseng, H. H.; Chiang, C. K. Improving the mechanical strength and gas separation performance of CMS membranes by simply sintering treatment of α -Al₂O₃ support. *J. Membr. Sci.* **2014**, *453*, 603–613.
- [64] Wey, M. Y.; Wang, C. T.; Lin, Y. T.; Lin, M. D.; Uchytil, P.; Setnickova, K.; Tseng, H. H. Interfacial interaction between CMS layer and substrate: Critical factors affecting membrane microstructure and H₂ and CO₂ separation performance from CH₄. *J. Membr. Sci.* **2019**, *580*, 49–61.
- [65] Li, J. Y.; Tseng, H. H.; Wey, M. Y. Tuning thermal expansion behavior and surface roughness of tubular Al₂O₃ substrates for fabricating high-performance carbon molecular sieving membranes for H₂ separation. *Int. J. Hydrol. Energy* **2019**, *44*, 24746–24758.
- [66] Lei, L. F.; Pan, F. J.; Lindbråthen, A.; Zhang, X. P.; Hillestad, M.; Nie, Y.; Bai, L.; He, X. Z.; Guiver, M. D. Carbon hollow fiber membranes for a molecular sieve with precise-cut-off ultramicropores for superior hydrogen separation. *Nat. Commun.* **2021**, *12*, 268.
- [67] Qiu, W. L.; Vaughn, J.; Liu, G. P.; Xu, L. R.; Brayden, M.; Martinez, M.; Fitzgibbons, T.; Wenz, G.; Koros, W. J. Hyperaging tuning of a carbon molecular-sieve hollow fiber membrane with extraordinary gas-separation performance and stability. *Angew. Chem., Int. Ed.* **2019**, *58*, 11700–11703.
- [68] Bunch, J. S.; Verbridge, S. S.; Alden, J. S.; van der Zande, A. M.; Parpia, J. M.; Craighead, H. G.; McEuen, P. L. Impermeable atomic membranes from graphene sheets. *Nano Lett.* **2008**, *8*, 2458–2462.
- [69] Koenig, S. P.; Wang, L. D.; Pellegrino, J.; Bunch, J. S. Selective molecular sieving through porous graphene. *Nat. Nanotechnol.* **2012**, *7*, 728–732.
- [70] Sun, P. Z.; Wang, K. L.; Zhu, H. W. Recent developments in graphene-based membranes: Structure, mass-transport mechanism and potential applications. *Adv. Mater.* **2016**, *28*, 2287–2310.
- [71] Kim, H. W.; Yoon, H. W.; Yoon, S. M.; Yoo, B. M.; Ahn, B. K.; Cho, Y. H.; Shin, H. J.; Yang, H.; Paik, U.; Kwon, S. et al. Selective gas transport through few-layered graphene and graphene oxide membranes. *Science* **2013**, *342*, 91–95.

- [72] Becerril, H. A.; Mao, J.; Liu, Z. F.; Stoltenberg, R. M.; Bao, Z. N.; Chen, Y. S. Evaluation of solution-processed reduced graphene oxide films as transparent conductors. *ACS Nano* **2008**, *2*, 463–470.
- [73] Shen, J.; Liu, G. P.; Huang, K.; Chu, Z. Y.; Jin, W. Q.; Xu, N. P. Subnanometer two-dimensional graphene oxide channels for ultrafast gas sieving. *ACS Nano* **2016**, *10*, 3398–3409.
- [74] Wang, X. R.; Chi, C. L.; Tao, J. F.; Peng, Y. W.; Ying, S. M.; Qian, Y. H.; Dong, J. Q.; Hu, Z. G.; Gu, Y. D.; Zhao, D. Improving the hydrogen selectivity of graphene oxide membranes by reducing non-selective pores with intergrown ZIF-8 crystals. *Chem. Commun.* **2016**, *52*, 8087–8090.
- [75] Wang, H.; Zhao, S.; Liu, Y.; Yao, R. X.; Wang, X. Q.; Cao, Y. H.; Ma, D.; Zou, M. C.; Cao, A. Y.; Feng, X. et al. Membrane adsorbers with ultrahigh metal-organic framework loading for high flux separations. *Nat. Commun.* **2019**, *10*, 4204.
- [76] Liu, Y. Y.; Ng, Z. F.; Khan, E. A.; Jeong, H. K.; Ching, C. B.; Lai, Z. P. Synthesis of continuous MOF-5 membranes on porous α -alumina substrates. *Microporous Mesoporous Mater.* **2009**, *118*, 296–301.
- [77] Guo, H. L.; Zhu, G. S.; Hewitt, I. J.; Qiu, S. L. “Twin copper source” growth of metal-organic framework membrane: $\text{Cu}_3(\text{BTC})_2$ with high permeability and selectivity for recycling H_2 . *J. Am. Chem. Soc.* **2009**, *131*, 1646–1647.
- [78] Bux, H.; Liang, F. Y.; Li, Y. S.; Cravillon, J.; Wiebcke, M.; Caro, J. Zeolitic imidazolate framework membrane with molecular sieving properties by microwave-assisted solvothermal synthesis. *J. Am. Chem. Soc.* **2009**, *131*, 16000–16001.
- [79] Liu, Q.; Wang, N. Y.; Caro, J.; Huang, A. S. Bio-inspired polydopamine: A versatile and powerful platform for covalent synthesis of molecular sieve membranes. *J. Am. Chem. Soc.* **2013**, *135*, 17679–17682.
- [80] Brown, A. J.; Johnson, J. R.; Lydon, M. E.; Koros, W. J.; Jones, C. W.; Nair, S. Continuous polycrystalline zeolitic imidazolate framework-90 membranes on polymeric hollow fibers. *Angew. Chem., Int. Ed.* **2012**, *51*, 10615–10618.
- [81] Wu, X. C.; Wei, W.; Jiang, J. W.; Caro, J.; Huang, A. S. High-flux high-selectivity metal-organic framework MIL-160 membrane for xylene isomer separation by pervaporation. *Angew. Chem., Int. Ed.* **2018**, *57*, 15354–15358.
- [82] Guo, H.; Liu, J. Q.; Li, Y. H.; Caro, J.; Huang, A. S. Post-synthetic modification of highly stable UiO-66-NH₂ membranes on porous ceramic tubes with enhanced H_2 separation. *Microporous Mesoporous Mater.* **2021**, *313*, 110823.
- [83] Liu, X. L.; Demir, N. K.; Wu, Z. T.; Li, K. Highly water-stable zirconium metal-organic framework UiO-66 membranes supported on alumina hollow fibers for desalination. *J. Am. Chem. Soc.* **2015**, *137*, 6999–7002.
- [84] Knebel, A.; Sundermann, L.; Mohmeyer, A.; Strauß, I.; Friebel, S.; Behrens, P.; Caro, J. Azobenzene guest molecules as light-switchable CO_2 valves in an ultrathin UiO-67 membrane. *Chem. Mater.* **2017**, *29*, 3111–3117.
- [85] Huang, A. S.; Chen, Y. F.; Wang, N. Y.; Hu, Z. Q.; Jiang, J. W.; Caro, J. A highly permeable and selective zeolitic imidazolate framework ZIF-95 membrane for H_2/CO_2 separation. *Chem. Commun.* **2012**, *48*, 10981–10983.
- [86] Ma, L.; Svec, F.; Tan, T. W.; Lv, Y. Q. *In-situ* growth of highly permeable zeolite imidazolate framework membranes on porous polymer substrate using metal chelated polyaniline as interface layer. *J. Membr. Sci.* **2019**, *576*, 1–8.
- [87] Xie, Z.; Yang, J. H.; Wang, J. Q.; Bai, J.; Yin, H. M.; Yuan, B.; Lu, J. M.; Zhang, Y.; Zhou, L.; Duan, C. Y. Deposition of chemically modified α -Al₂O₃ particles for high performance ZIF-8 membrane on a macroporous tube. *Chem. Commun.* **2012**, *48*, 5977–5979.
- [88] Zhang, X. F.; Liu, Y. G.; Li, S. H.; Kong, L. Y.; Liu, H. O.; Li, Y. S.; Han, W.; Yeung, K. L.; Zhu, W. D.; Yang, W. S. et al. New membrane architecture with high performance: ZIF-8 membrane supported on vertically aligned ZnO nanorods for gas permeation and separation. *Chem. Mater.* **2014**, *26*, 1975–1981.
- [89] Nian, P.; Cao, Y.; Li, Y. J.; Zhang, X.; Wang, Y. L.; Liu, H. O.; Zhang, X. F. Preparation of a pure ZIF-67 membrane by self-conversion of cobalt carbonate hydroxide nanowires for H_2 separation. *CrystEngComm* **2018**, *20*, 2440–2448.
- [90] Drobek, M.; Bechelany, M.; Vallicari, C.; Abou Chaaya, A.; Charmette, C.; Salvador-Levehang, C.; Miele, P.; Julbe, A. An innovative approach for the preparation of confined ZIF-8 membranes by conversion of ZnO ALD layers. *J. Membr. Sci.* **2015**, *475*, 39–46.
- [91] Zhou, S.; Wei, Y. Y.; Zhuang, L. B.; Ding, L. X.; Wang, H. H. Introduction of metal precursors by electrodeposition for the *in situ* growth of metal-organic framework membranes on porous metal substrates. *J. Mater. Chem. A* **2017**, *5*, 1948–1951.
- [92] Ma, X. X.; Li, Y. H.; Huang, A. S. Synthesis of nano-sheets seeds for secondary growth of highly hydrogen permselective ZIF-95 membranes. *J. Membr. Sci.* **2020**, *597*, 117629.
- [93] Zhong, Z. X.; Yao, J. F.; Chen, R. Z.; Low, Z.; He, M.; Liu, J. Z.; Wang, H. T. Oriented two-dimensional zeolitic imidazolate framework-L membranes and their gas permeation properties. *J. Mater. Chem. A* **2015**, *3*, 15715–15722.
- [94] Ranjan, R.; Tsapatsis, M. Microporous metal organic framework membrane on porous support using the seeded growth method. *Chem. Mater.* **2009**, *21*, 4920–4924.
- [95] Shamsaei, E.; Lin, X. C.; Low, Z. X.; Abbasi, Z.; Hu, Y. X.; Liu, J. Z.; Wang, H. T. Aqueous phase synthesis of ZIF-8 membrane with controllable location on an asymmetrically porous polymer substrate. *ACS Appl. Mater. Interfaces* **2016**, *8*, 6236–6244.
- [96] Huang, K.; Li, Q. Q.; Liu, G. P.; Shen, J.; Guan, K. C.; Jin, W. Q. A ZIF-71 hollow fiber membrane fabricated by contra-diffusion. *ACS Appl. Mater. Interfaces* **2015**, *7*, 16157–16160.
- [97] Yao, J. F.; Dong, D. H.; Li, D.; He, L.; Xu, G. S.; Wang, H. T. Contra-diffusion synthesis of ZIF-8 films on a polymer substrate. *Chem. Commun.* **2011**, *47*, 2559–2561.
- [98] Stassen, I.; Styles, M.; Grenci, G.; Van Gorp, H.; Vanderlinden, W.; De Feyter, S.; Falcaro, P.; De Vos, D.; Vereecken, P.; Ameloot, R. Chemical vapour deposition of zeolitic imidazolate framework thin films. *Nat. Mater.* **2016**, *15*, 304–310.
- [99] Nian, P.; Liu, H. O.; Zhang, X. F. Bottom-up fabrication of two-dimensional Co-based zeolitic imidazolate framework tubular membranes consisting of nanosheets by vapor phase transformation of Co-based gel for H_2/CO_2 separation. *J. Membr. Sci.* **2019**, *573*, 200–209.
- [100] Hou, Q. Q.; Wu, Y.; Zhou, S.; Wei, Y. Y.; Caro, J.; Wang, H. H. Ultra-tuning of the aperture size in stiffened ZIF-8-Cm frameworks with mixed-linker strategy for enhanced CO_2/CH_4 separation. *Angew. Chem., Int. Ed.* **2019**, *58*, 327–331.
- [101] Zhou, S.; Wei, Y. Y.; Li, L. B.; Duan, Y. F.; Hou, Q. Q.; Zhang, L. L.; Ding, L. X.; Xue, J.; Wang, H. H.; Caro, J. Paralyzed membrane: Current-driven synthesis of a metal-organic framework with sharpened propene/propane separation. *Sci. Adv.* **2018**, *4*, eaau1393.
- [102] Kim, J. O.; Koo, W. T.; Kim, H.; Park, C.; Lee, T.; Hutomo, C. A.; Choi, S. Q.; Kim, D. S.; Kim, I. D.; Park, S. Large-area synthesis of nanoscopic catalyst-decorated conductive MOF film using microfluidic-based solution shearing. *Nat. Commun.* **2021**, *12*, 4294.
- [103] Liu, L. L.; Song, Y. F.; Ji, T. T.; Sun, Y. W.; He, D. M.; Hu, H. Q.; Liu, Y. Beyond solution-based protocols: MOF membrane synthesis in supercritical environments for an elegant sustainability performance balance. *ACS Mater. Lett.* **2020**, *2*, 1142–1147.
- [104] Peng, Y.; Li, Y. S.; Ban, Y. J.; Jin, H.; Jiao, W. M.; Liu, X. L.; Yang, W. S. Metal-organic framework nanosheets as building blocks for molecular sieving membranes. *Science* **2014**, *346*, 1356–1359.
- [105] Ma, Y. N.; Zhang, W.; Li, H. Y.; Zhang, C. C.; Pan, H. M.; Zhang, Y. F.; Feng, X. S.; Tang, K. W.; Meng, J. Q. A microporous polymer TFC membrane with 2-D MOF nanosheets gutter layer for efficient H_2 separation. *Sep. Purif. Technol.* **2021**, *261*, 118283.
- [106] Cheng, L.; Yang, H. N.; Chen, X. Y.; Liu, G. Z.; Guo, Y. N.; Liu, G. P.; Jin, W. Q. MIL-101(Cr) microporous nanocrystals intercalating graphene oxide membrane for efficient hydrogen purification. *Chem. Asian J.* **2021**, *16*, 3162–3169.
- [107] Cheng, L.; Guan, K. C.; Liu, G. P.; Jin, W. Q. Cysteamine-crosslinked graphene oxide membrane with enhanced hydrogen separation property. *J. Membr. Sci.* **2020**, *595*, 117568.



Ahui Hao is current a PhD candidate in the School of Materials Science and Engineering, Beihang University. Her research focuses on the design and fabrication of MOF-base materials in gas separation and energy conversion.



Prof. Jianglan Shui received one PhD degree from University of Science and Technology of China (2006) and one from University of Rochester (2010). He worked as a postdoctor at Argonne National Laboratory (2010–2013) and Case Western Reserve University (2013–2014). He joined School of Materials Science and Engineering at Beihang University in 2015. Prof. Shui's research focuses on key materials and devices for hydrogen energy, including electrocatalysts, hydrogen storage materials, and proton exchange membrane fuel cells.